

EXPERIMENTAL ELASTIC DEFORMATION CHARACTERIZATION OF A FLAPPING-WING MAV USING VISUAL IMAGE CORRELATION

Kelly Stewart
Air Force Research Laboratory
Munitions Directorate
AFRL/RWGN
Eglin AFB, FL 32542-6810

Roberto Albertani
University of Florida
Research and Engineering Education Facility
Shalimar, FL 32579



NOVEMBER 2007

CONFERENCE PAPER

This paper was presented at the Critical Technology Development for Micro Munition Vehicles, TTCP Meeting, held at Aberdeen Proving Ground, MD; 16-17 October 2007. One of the authors is a U.S. Government employee working within the scope of her position; therefore, the U.S. Government is joint owner of the work. If published, the publisher may assert copyright. If so, the U.S. Government has the right to copy, distribute, and use the work by or on behalf of the U.S. Government. Any other form of use is subject to copyright restrictions.

This paper is published in the interest of the scientific and technical information exchange. Publication of this paper does not constitute approval or disapproval of the ideas or findings.

DISTRIBUTION A: Approved for public release; distribution unlimited.
Approval Confirmation #AAC/PA 10-11-07-596; dated 11 October 2007.

AIR FORCE RESEARCH LABORATORY, MUNITIONS DIRECTORATE

■ Air Force Materiel Command ■ United States Air Force ■ Eglin Air Force Base

REPORT DOCUMENTATION PAGE
*Form Approved
OMB No. 0704-0188*

The public reporting burden for this collection of information is estimated to average 1 hour per response, including the time for reviewing instructions, searching existing data sources, gathering and maintaining the data needed, and completing and reviewing the collection of information. Send comments regarding this burden estimate or any other aspect of this collection of information, including suggestions for reducing the burden, to Department of Defense, Washington Headquarters Services, Directorate for Information Operations and Reports (0704-0188), 1215 Jefferson Davis Highway, Suite 1204, Arlington, VA 22202-4302. Respondents should be aware that notwithstanding any other provision of law, no person shall be subject to any penalty for failing to comply with a collection of information if it does not display a currently valid OMB control number.

PLEASE DO NOT RETURN YOUR FORM TO THE ABOVE ADDRESS.

1. REPORT DATE (DD-MM-YYYY)	2. REPORT TYPE	3. DATES COVERED (From - To)		
4. TITLE AND SUBTITLE		5a. CONTRACT NUMBER		
		5b. GRANT NUMBER		
		5c. PROGRAM ELEMENT NUMBER		
6. AUTHOR(S)		5d. PROJECT NUMBER		
		5e. TASK NUMBER		
		5f. WORK UNIT NUMBER		
7. PERFORMING ORGANIZATION NAME(S) AND ADDRESS(ES)			8. PERFORMING ORGANIZATION REPORT NUMBER	
9. SPONSORING/MONITORING AGENCY NAME(S) AND ADDRESS(ES)			10. SPONSOR/MONITOR'S ACRONYM(S)	
			11. SPONSOR/MONITOR'S REPORT NUMBER(S)	
12. DISTRIBUTION/AVAILABILITY STATEMENT				
13. SUPPLEMENTARY NOTES				
14. ABSTRACT				
15. SUBJECT TERMS				
16. SECURITY CLASSIFICATION OF:		17. LIMITATION OF ABSTRACT	18. NUMBER OF PAGES	19a. NAME OF RESPONSIBLE PERSON
a. REPORT	b. ABSTRACT	c. THIS PAGE		19b. TELEPHONE NUMBER (Include area code)

Experimental Elastic Deformation Characterization of a Flapping-Wing MAV using Visual Image Correlation

KTA 2-25-06, TTCP WPN-2

16 October 2007



**DISTRIBUTION A: Approved for public release; distribution unlimited.
Approval Confirmation #AAC/PA 10-11-07-596.**

**Ms. Kelly Stewart
Air Force Research Laboratory
Munitions Directorate
Eglin AFB, FL**

**Dr. Roberto Albertani
University of Florida
Research and Engineering Education Facility
Shalimar, FL**

This presentation will detail AFRL/MN's collaboration with the University of Florida to derive a method for estimating elastic deformation in flexible, flapping wings. By knowing the elastic deformation that occurs, researchers can better understand the mechanics and aerodynamic effects behind flexible, flapping wings and apply that knowledge to various design aspects of micro air vehicles (MAV's) such as wing structure, guidance and control, etc.



Overview



- **Introduction / Motivation**
- **Methodology**
- **Validation**
- **Dynamic Tests**
 - **Setup**
 - **Post-processing**
- **Results**
 - **Wing Motion**
 - **Uncertainty in Rotation Angle**
 - **Wing Deformation**
- **Conclusion / Future Work**

Approved for public release; Distribution Unlimited. 10-11-07-596

2

Here is an overview of my presentation. I will first discuss the background of this research and explain why flexible, flapping wings are of interest to the research community.

I will then explain the method of using a dynamic visual-image-correlation (VIC) system to capture wing deformation and briefly describe a validation test used to gain confidence in the post-processing algorithm.

Following the validation results, I will present a series of dynamic tests involving two flapping wings, each of different structure and material.

I will conclude with a summary of the test results and future work involving the use of the method presented.



Introduction



- **Interest in research community to further develop MAV technology for performance in tightly confined environments at varying flight conditions**
- **Biological Inspiration**
 - **Flexible wings**
 - Can readily adopt to changing flight conditions
 - Fixed-wing MAVs whose wing structures are fabricated from aeroelastic material show improvement over rigid counterparts
 - **Flapping wings**
 - Flexible, fixed-wings show an advantage, but still do not meet all of the agility and versatility requirements
 - Natural fliers (bats, birds, insects) use flapping motion at low speed



Copyright Jamie Gundry 2004

Approved for public release; Distribution Unlimited. 10-11-07-596

3

The use of MAVs within tightly confined environments under widely varying flight conditions is generating much interest in the research community. Such application of MAVs will require them to be highly agile and adaptable, much like the natural fliers we see today.

A common characteristic of natural fliers at low-speeds is wing flexibility. This flexibility allows fliers to readily adopt to changing flight conditions, either through passive mechanisms such as adaptive washout or by active morphing of the wing shape to increase lift. In the case of fixed-wing MAVs, designs involving wings made from an aeroelastic material show an improvement in the pitching moment curve and the ability to store energy that would normally be lost to wing-tip vortices and wake.

While flexible, fixed-wings do show an advantage over their rigid counterparts, they still do not meet all of the agility and versatility requirements for low-speed flight in constricted environments. Biology has shown that natural fliers who fly at low speeds use flapping rather than fixed-wings. This is seen in birds, bats, and insects. The video in the bottom left corner shows a fly in flight. Notice how flexible its wings are by the large deformations that occur during the flapping motion.



Motivation



- Worth investigating kinematics and dynamics of flapping motion
- Kinematics and dynamics must be decoupled when applying biologically-inspired technologies
 - Only rigid-body-motion is needed for IMU and system identification
 - However, combining wing mechanics of flexible wings with feedback control requires knowing elastic deformation
- Dynamic visual image correlation (VIC) enables simultaneous measurement of rigid-body-motion and deformation

Approved for public release; Distribution Unlimited. 10-11-07-596

4

With the examples that exist of natural fliers exploiting flexible, flapping wings, it is worth investigating the kinematics and dynamics of such motion.

The wing kinematics and dynamics need to be decoupled when applying biologically inspired technologies to MAVs. For instance, while the inertial measurement unit and system identification only require knowing the rigid-body-motion, the same is not true for feedback control. Combining the wing mechanics of flexible wings with feedback control similar to that seen in biological organisms requires knowing the elastic deformation.

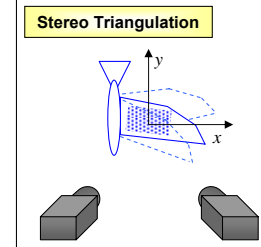
A dynamic VIC system provides a means for simultaneously measuring both rigid-body-motion and deformation and is already being used extensively on flexible, fixed-wing MAVs as documented by a University of Florida colleague, Dr. Roberto Albertani. This presentation will detail a method for setting up flapping-wing VIC experiments and estimating the elastic deformation using the data obtained.



Methodology



- VIC measures full-field displacements through stereo triangulation
 - Provides reference points (X, Y, Z)
 - Provides displacement measurements (u, v, w)
 - Displacement is result of both kinematics and deformation
- Deformation is difference between total displacement and rigid body displacement



$$\begin{bmatrix} u_{Elastic} \\ v_{Elastic} \\ w_{Elastic} \\ 1 \end{bmatrix}_i^{\hat{x}, \hat{y}, \hat{z}} = \begin{bmatrix} X + u \\ Y + v \\ Z + w \\ 1 \end{bmatrix}_i^{\hat{x}, \hat{y}, \hat{z}} - [HTM] \begin{bmatrix} X \\ Y \\ Z \\ 1 \end{bmatrix}_i^{\hat{x}, \hat{y}, \hat{z}}$$

- Acquire rigid body displacement by deriving homogeneous transformation matrix (HTM)

Approved for public release; Distribution Unlimited. 10-11-07-596

5

VIC uses stereo triangulation to measure in-plane and out-of-plane displacements for a test specimen undergoing any type of motion. Stereo triangulation involves focusing two high-speed cameras positioned at different angles with respect to the test specimen. The cameras record a series of images and perform a correlation between the two sets to arrive at the displacement. In order for the stereo triangulation to take place, the test specimen must be covered in a random, speckled pattern with very little glare. Data that is returned from the VIC includes the initial starting position (X,Y,Z) and the displacement at each time step (u,v,w).

The measured displacement is the sum of both the wing kinematics and wing deformation. The wing kinematics is synonymous to the rigid-body-motion of the wing. If the rigid-body-motion can be determined, then the wing deformation can be found by subtraction (as displayed in the equation).

The rigid-body-motion is described by the homogeneous transformation matrix, which is used by image processing to define rotation, translation, perspective, and scaling. For a test specimen such as a flapping wing, the homogenous transformation matrix varies with time and must be solved for at each time step.



Rigid-body-motion from HTM



- Motion based on AOI frame of reference

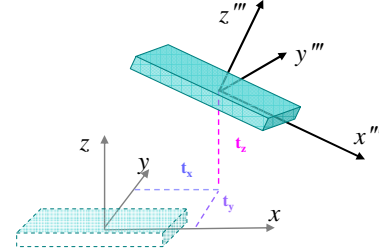
- Rotation

- Flapping angle, $\Gamma \rightarrow R_y$
 - Sweep angle, $\Psi \rightarrow R_z$
 - Feather angle, $\Theta \rightarrow R_x$

- Translation (t_x , t_y , t_z)

- Homogeneous Transformation Matrix

$$HTM = \begin{bmatrix} c\Gamma c\Psi & -s\Psi & s\Gamma c\Psi & t_x \\ c\Gamma s\Psi c\Theta + s\Gamma s\Theta & c\Psi c\Theta & s\Gamma s\Psi c\Theta - c\Gamma s\Theta & t_y \\ c\Gamma s\Psi s\Theta - s\Gamma c\Theta & c\Psi s\Theta & s\Gamma s\Psi s\Theta + c\Gamma c\Theta & t_z \\ 0 & 0 & 0 & 1 \end{bmatrix}$$



$$[\bar{Z} + \bar{W}]_{N \times 1} = [\bar{X} \quad \bar{Y} \quad \bar{Z}]_{N \times 4} \begin{bmatrix} HTM_{31} \\ HTM_{32} \\ HTM_{33} \\ HTM_{34} \end{bmatrix}_{4 \times 1}$$

- Setup problem in form $[b] = [A] [x]$ and solve for $[x]$

- $[b]$ = VIC measurements
 - $[A]$ = known reference points (X,Y,Z)
 - $[x]$ = coefficients of the transformation matrix

$$\Theta = \tan^{-1}\left(\frac{HTM_{23}}{HTM_{22}}\right)$$

$$\Psi = \tan^{-1}\left(\frac{-HTM_{12}}{c\Gamma \cdot HTM_{22} + s\Gamma \cdot HTM_{32}}\right)$$

$$\Gamma = \tan^{-1}\left(\frac{-c\Theta \cdot HTM_{31} + s\Theta \cdot HTM_{21}}{HTM_{11} / c\Psi}\right)$$

Approved for public release; Distribution Unlimited. 10-11-07-596

6

The VIC system uses a coordinate system where in-plane motion occurs along the x-axis and y-axis, out-of-plane motion occurs along the z-axis. For an arbitrarily selected area on a flapping wing mounted vertically to the cameras, the flapping angle refers to the rotation about the y-axis. The rotation about the x-axis is referred to as the feathering angle and about the z-axis is the sweep angle. If the area of interest (AOI) happens to be offset from the origin, then a corresponding translation occurs with the rotation.

Premultiplying the rotation matrices and translation matrix results in the complete HTM shown. The measured displacements from the VIC, for each time step, are equal to the initial starting points (X,Y,Z) multiplied by the HTM for that time step.

The HTM is solved for by applying a linear least-squares regression across the points making up the AOI. This finds the HTM that yields the best fit to the measured displacements. Once the elements comprising the HTM are known, inverse trigonometry is applied to get the rotation angles. Again, this calculation is performed for each time step since the specimen is moving.

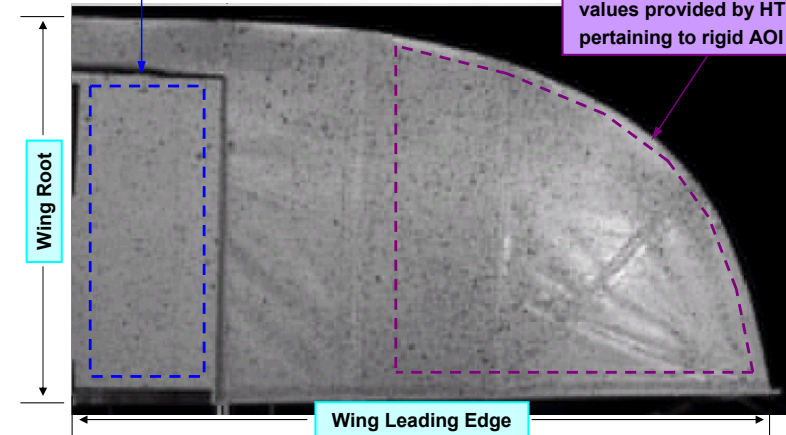


Area of Interest



Rigid AOI

- Follows flapping motion
- Provides displacement data from which HTM will be derived



Flexible AOI

- Displacement is combination of rotation, translation, and deformation
- Rotation and translation values provided by HTM pertaining to rigid AOI

Approved for public release; Distribution Unlimited. 10-11-07-596

7

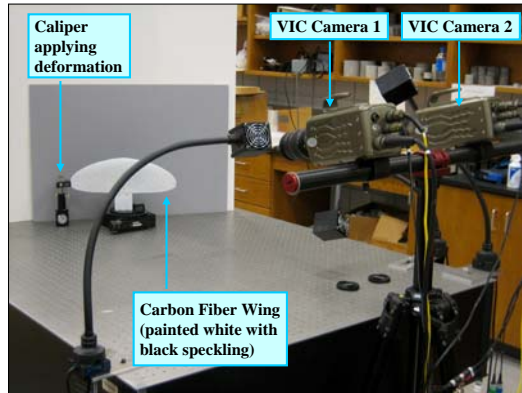
This picture provides an example of a rigid AOI and flexible AOI on a test specimen. The inboard section of the wing shown here has a rigid plate (in this case, a piece of balsa wood) that provides the rigid AOI. This plate is positioned to follow the movement of the wing while interfering as little as possible with any deformation that may occur. Further out is the flexible AOI. VIC data is acquired for the entire wing surface, but the two AOIs are mapped out and processed separately, with the rigid AOI providing the HTM estimate.



Validation Tests

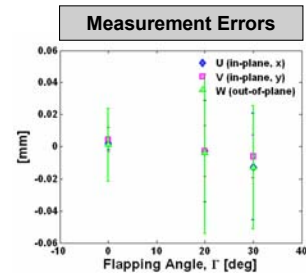


- Subjected carbon fiber wing to known rotations and deformations
- Repetition tests at 0° with no deformation → acquire measurement uncertainties



Estimate Errors	
Rotation, Γ°	Deformation (mm)*
0.2	0.3 – 0.9

* Note: AOI did not extend completely to wing tip



Approved for public release; Distribution Unlimited. 10-11-07-596

8

To check the feasibility of such a method, a simple validation test was performed for a combination of known rotations and deformations. A carbon fiber wing was rotated on a stand to some set flapping angle. Calibers, mounted vertically and fixed to the table, were used to apply a deformation at the wing tip. The estimated flapping angle was in error of 0.2° or less. The deformation estimates ranged in error from 0.3 mm to 0.9 mm, however, the AOI used during processing did not extend out to the wing tip due to correlation issues near the wing edge.

Measurement errors for the test setup were acquired by taking 50 snapshots of the wing held fixed at 0 degrees rotation and no deformation. The resulting errors were on the order of 0.01 mm or less, which was considered acceptable.



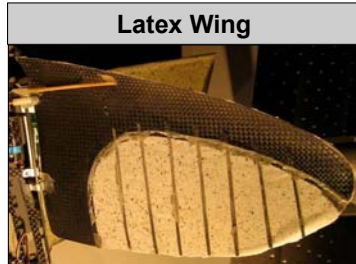
Dynamic Tests



- Two wings of different material subjected to flapping motion



Kite Wing



Latex Wing

<ul style="list-style-type: none">• Acquired from commercial vehicle capable of flapping flight• Kite-like material does not stretch• Carbon fiber rods	<ul style="list-style-type: none">• Fabricated at the UF MAV Lab• Thin latex (0.33 mm thick) stretches significantly• Wing perimeter is bidirectional carbon fiber• Battens are unidirectional carbon fiber
---	--

Approved for public release; Distribution Unlimited. 10-11-07-596

9

Having validated the method as feasible, a series of dynamic tests are conducted using two different types of wings.

The first wing is from a commercially available vehicle that is capable of flapping flight. A green kite-like material, that does not stretch, is placed over a framework of carbon fiber rods to form the wing. This wing is referred to as the kite wing.

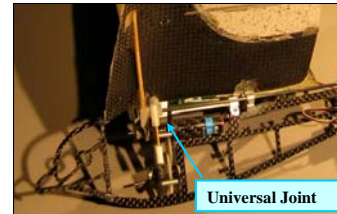
The second wing was fabricated at the University of Florida MAV Lab. It is comprised of a thin latex membrane stretched between a carbon fiber perimeter. This wing is referred to as the latex wing.



Test Setup



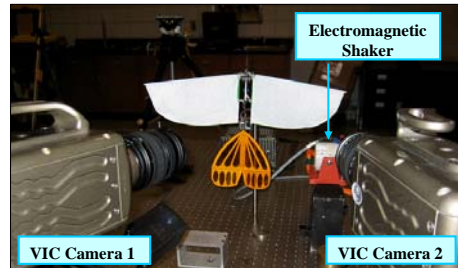
- Rigid plate affixed to inboard section of wing
- Wing attached to linear actuator via a rigid rod and universal joint with low friction
- Sinusoidal signal fed to linear actuator at 5 Hz and 10 Hz
- Load cell placed between the wing and the linear actuator
- Data recorded for 1 sec at 100 fps



Universal Joint

Electromagnetic Shaker
(Linear Actuator)
Ling Dynamic Systems
V201/3-PA 25E
Frequencies up to
13,000 Hz

Load Cell
Brüel & Kier
8230
Sensitivity of
110 mV/N



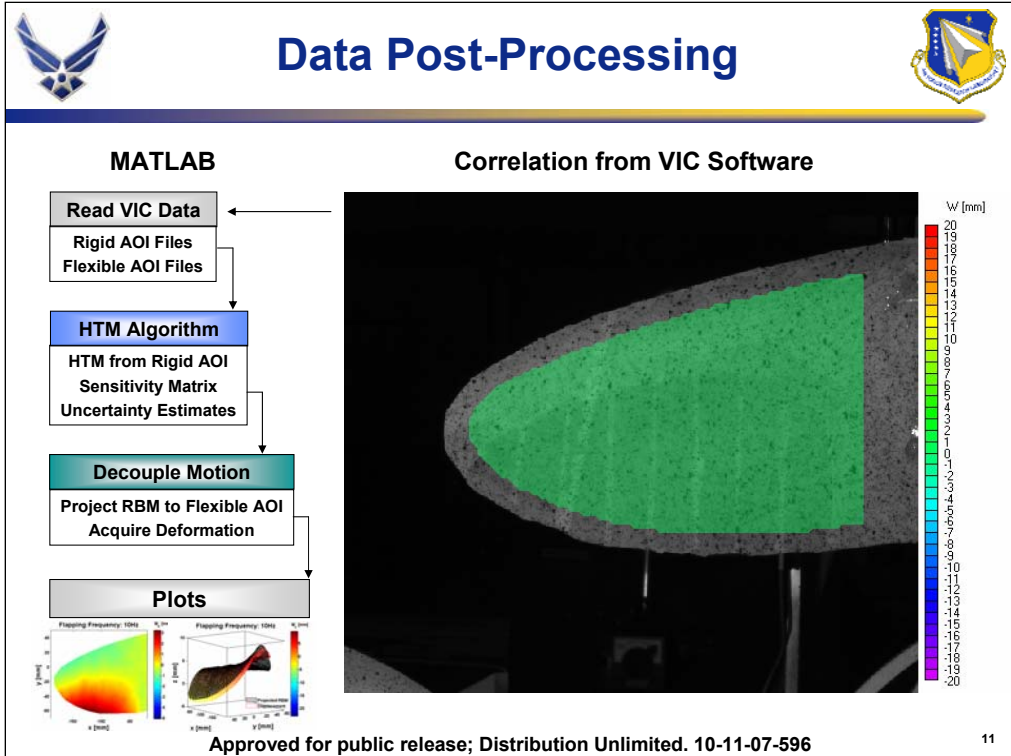
Approved for public release; Distribution Unlimited. 10-11-07-596

10

In order for the HTM to be derived, a rigid area on the wing specimen is needed. This is accomplished by affixing a rigid plate to the inboard section of the wing. The plate is attached in such a way as to interfere as little as possible with any deformation that may occur. Rather, the plate's sole purpose is to simply move with the wing so that the rotation angles can be estimated.

A linear actuator is attached to the wing via a rigid rod and universal joint, as shown in the top right picture. A sinusoidal signal sent to the actuator generates the flapping motion. Between the actuator and the wing specimen is a load cell, which adjusts the amplitude of the input signal to stay within acceleration limits. Two flapping frequencies were tested: 5 Hz and 10 Hz. For each test, 1 second's worth of data was recorded at 100 frames per second.

The bottom right picture shows a test setup with the kite wing. The two VIC cameras can be seen as well as the electromagnetic shaker which acted as the linear actuator.



Once a test is complete, the VIC software performs the stereo triangulation across the recorded images. The movie to the right shows a series of images recorded by the VIC. The colored area is the correlated AOI specified by the user. The color bands indicate the measured out-of-plane displacement. If the wing specimen were completely rigid, the color bands would remain as vertical lines of color moving from the wing root to the wing tip. However, it is evident some wing deformation is occurring by the distortion of the bands during the transitions from upstroke to downstroke and vice versa.

The VIC data is fed into a MATLAB program for post-processing. Two sets of files are processed simultaneously: one set for the rigid AOI (the rigid plate located on the inboard section of the wing) and a flexible AOI located out towards the wing tip. Data for both AOIs come from the same VIC images. The rigid AOI files provide the HTM at each time step, which is then used to project the rigid-body-motion out towards the flexible AOI. After this, the wing motion can be decoupled and the wing deformation at each time step is arrived at.

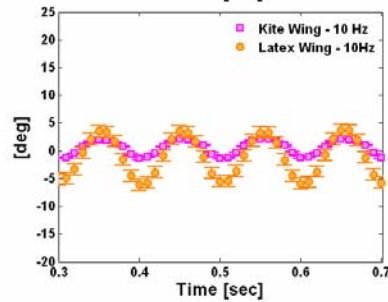
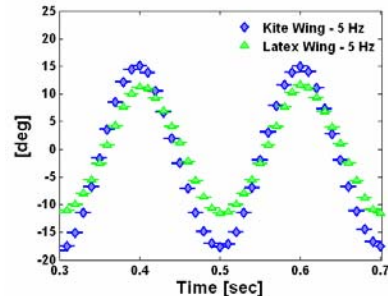
The MATLAB program also calculates the sensitivity of the rotation angles to errors in the estimated HTM. This provides a means for tracking the error propagation.



Results – Wing Motion



- Acquired time history of flapping angle
 - Amplitude was adjusted by load cell to stay within acceleration limits
- Kite wing
 - Amplitude: 16.5° at 5 Hz
 2.0° at 10 Hz
- Latex wing
 - Amplitude: 12.0° at 5 Hz
 4.5° at 10 Hz
 - Estimates at 10 Hz have largest uncertainty of all tests



	5 Hz	10 Hz
Kite Wing	$1.06\text{e-}02^\circ$	$8.94\text{e-}03^\circ$
Latex Wing	$1.68\text{e-}03^\circ$	1.01°

Approved for public release; Distribution Unlimited. 10-11-07-596

12

Upon processing the VIC data through the MATLAB program, the following time histories of the flapping angle are acquired. The upper right plot shows the time history for the two wings at the 5 Hz frequency. The bottom right plot shows the time history for the two wings at the 10 Hz frequency. The difference in maximum flapping angle between each of the cases is a result of structural differences between the two wings and the adjustment of the input signal amplitude by the load cell.

The estimated uncertainty for each test case is shown in the bottom table. Notice that the latex wing flapping at 10 Hz has a rather large uncertainty with respect to the other cases. This is due to error propagation from the estimated HTM and is explained on the next slide.



Results – Uncertainty in Estimates



- **Coefficients pertaining to very small X, Y, or Z values will have a larger uncertainty**
 - Result of model used in linear regression
 - Algorithm initially assumed Z would be small compared to X, Y
 - Performs inverse trigonometry with the first two columns of the HTM
 - Uncertainty in flapping angle is a function of $u_{HTM,11}, u_{HTM,21}, u_{HTM,31}, u_{HTM,\theta}, u_{HTM,\psi}$
 - Correlated rigid AOI for latex wing at 10 Hz, however, had small values for X as well

$$u_{HTM} = \begin{bmatrix} u_u/X & u_u/Y & u_u/Z & u_u \\ u_v/X & u_v/Y & u_v/Z & u_v \\ u_w/X & u_w/Y & u_w/Z & u_w \\ - & - & - & - \end{bmatrix}$$

$$u_{HTM,L10} = \begin{bmatrix} 1.68e-02 & -1.71e-05 & 7.94e-03 & 2.75e-03 \\ -2.26e-03 & 2.30e-06 & -1.07e-03 & -3.70e-04 \\ -1.77e-02 & 1.08e-05 & -8.36e-03 & -2.89e-03 \\ -- & -- & -- & -- \end{bmatrix}$$

Approved for public release; Distribution Unlimited. 10-11-07-596

13

Recall, the HTM is estimated by using linear regression to find the matrix values which, when multiplied with the reference points (X, Y, Z), yield the best fit to the measured displacements. The smaller the values of X, Y, and Z, the larger the uncertainty in the HTM estimate. Sometimes, it was not possible to get a good correlation over the entire rigid plate and only a small area of the plate could actually be used to estimate the HTM. If this area was particularly narrow along the X or Y axis, then any elements of the HTM that correspond to that axis will have large uncertainties.

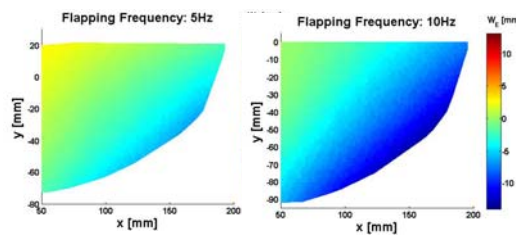
This happened to be the case with the latex wing at 10 Hz. The rigid AOI for this case was very narrow along the x-axis, thus, all the HTM elements in the first column of the HTM had large uncertainties. The initial HTM algorithm did not account for this, so the uncertainty propagated throughout the rest of the post-processing to result in a relatively large value of 1°. This was a lesson learned and can be avoided by having the MATLAB program perform a check on the HTM uncertainties prior to proceeding with calculations.



Results – Kite Wing Deformation



Start of Upstroke



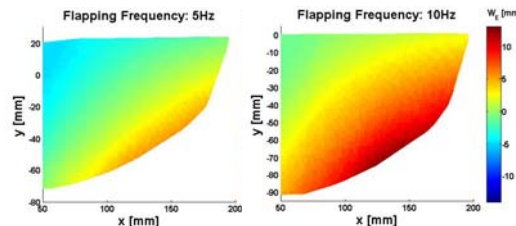
- **Out-of-plane only**

- Unidirectional contour bands
- Small amount of wing twist

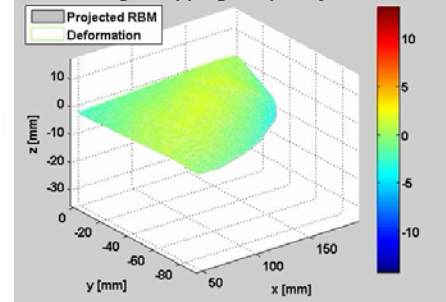
- **Maximum deformation**

- ± 5 mm at 5 Hz
- ± 12 mm at 10Hz

Start of Downstroke



Kite Wing - Flapping Frequency: 10Hz



Approved for public release; Distribution Unlimited. 10-11-07-596

14

The final outputs of the HTM algorithm consist of contour and 3-dimensional plots showing the wing deformation and wing kinematics. Presented here are the results for the kite wing.

The top contour plots show the amount of wing deformation at the start of the upstroke for both the 5 Hz and 10 Hz test cases. The bottom contour plots show the deformation at the start of the downstroke. The contour bands maintain a uniform direction across the wing surface as would be expected for a material that only experiences out-of-plane deformation.

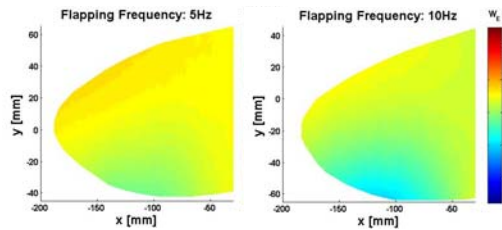
In the bottom right of the slide is a movie showing the rigid-body-motion of the wing, the black mesh, alongside the wing deformation, the colored mesh. Notice the wing twist captured in the deformation.



Results – Latex Wing Deformation



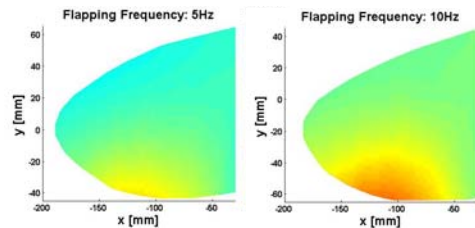
Start of Upstroke



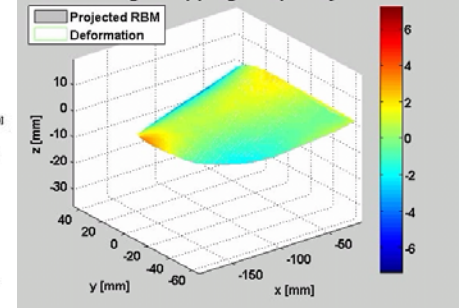
- In-plane and out-of-plane
 - Circular contour bands
 - Small amount of wing twist

- Maximum Deformation
 - ± 3 mm at 5 Hz
 - ± 5 mm at 10Hz

Start of Downstroke



Latex Wing - Flapping Frequency: 10Hz



Approved for public release; Distribution Unlimited. 10-11-07-596

15

Here are the results for the latex wing. Just as on the previous slide, the top contour plots refer to the deformation at the start of the upstroke and the bottom contour plots show the deformation at the start of the downstroke. The contours consist of circular bands due to the combination of both in-plane and out-of-plane deformation. Interestingly, even though the latex wing material had significant stretch compared to that of the kite wing material, the magnitude of deformation was less. This is most likely due to the different structure of the wing.

Again, the movie in the bottom right shows both the rigid-body-motion of the wing and the wing deformation. The wing twist seems to be more pronounced versus that of the kite wing, though it is uncertain whether this is due to larger inertial forces or larger aerodynamic forces. Since each test case experienced a different amplitude in flapping angle and the wings each had different structures and materials, no strong conclusions with regard to the influence of aerodynamic versus inertial forces can be drawn. Rather, the point of the dynamic experiment was to further test the HTM algorithm against time-varying data and increase confidence in its calculations.



Conclusion



- **Method for decoupling the wing kinematics from the deformation of a flapping-wing using VIC data**
 - Constructed HTM from rigid-body-motion and projected to flexible AOI → subtracted to get deformation
 - Provided time history of flapping angle and contour plots
 - Observed that a careful check of HTM uncertainties should be carried out prior to projecting RBM
- **Future work**
 - Dynamic VIC in conjunction with wind tunnel testing
 - Can the corresponding change in aerodynamics with wing shape be quantified?
 - Study of wing deformation in vacuum
 - How much of the deformation is related to inertial forces versus aerodynamic loads?

Approved for public release; Distribution Unlimited. 10-11-07-596

16

In conclusion, a method has been shown that decouples displacements measured by a VIC system into wing kinematics and wing deformation. It accomplishes this by constructing the HTM for a rigid part of the wing that is either inherent or artificially placed and, thus, acquiring the rigid-body-motion of the wing itself.

By calculating the HTM at every time step, the kinematic motion of the wing over time can be acquired. This is plotted in the time histories of three rotational angles: flapping, feathering, and sweep. The algorithm also captures the contour plots over time, providing insight into the magnitude and direction of wing deformation across the AOI.

Future work with this algorithm would involve processing VIC data acquired simultaneously along with sting balance data in a wind tunnel. This could possibly give insight into the behavior of the aerodynamics for a flapping wing.

Another study using this algorithm would involve comparing flapping-wing deformation within a vacuum versus that at atmospheric pressure to determine how much of the deformation is due to inertial forces versus aerodynamic loads. Experimental work, both with the wind tunnel and vacuum chamber, would be conducted by Dr. Roberto Albertani of the University of Florida. It is anticipated that AFRL / RWGN would continue to collaborate with Dr. Albertani during these studies as the work will be beneficial to on-going MAV research.